Numerical Simulations of Chaotic Mixing

B.T. Tan, P. Morris, M.C. Thompson and K. Hourigan
Dept. of Mechanical Engineering, Monash University, Clayton, Victoria

ABSTRACT

Numerical simulations of high Reynolds number flows in the unit driven cavity have been performed. The system is shown to become unsteady at $Re = 8,125$ and chaotic at $Re = 17,000$. In between this range the system switches between periodic and quasi-periodic states with step-wise changes in period. A passive concentration field is introduced to the flow at its asymptotic state to show the effects of chaos on mixing.

NOMENCLATURE

A	area
c	passive concentration field
c_0	initial passive concentration field
p	pressure
Pe	Peclet number
t	dimensionless time
$\mathbf{u}$	velocity vector
$\mathbf{u}^*, \mathbf{u}^{**}$	intermediate velocity vector
$\mathbf{u}'$	perturbed velocity vector
Re	Reynolds number
ϵ	small constant

1. INTRODUCTION

Mixing of fluids is important in many industrial and environmental situations, but because the process is poorly understood, most studies are postdictive rather than predictive. Improving efficiency is obviously an industrial imperative as costs increase with power input and length of time required for fluids to be sufficiently mixed. However, in any generalised case, many factors can be changed individually or in combination, and it is the identification of the dominant factors and modifications which lead to greater mixing efficiency.

Although full mixing vessel designs can now be studied numerically, there are advantages to gain an understanding at a basic level and using this knowledge to suggest improvements. In the current study, most of the geometrical detail has been removed, and the mixing properties of the system are examined as the governing parameters are altered. A basic prototype of a mixer is the driven cavity flow, since it contains the essential feature of one of the walls providing a shearing force to drive the fluid within the regime, thus representing some level of mechanical agitation. Even within such a simple system however, four distinct flow regimes have been found. The transition from steady to chaotic flow, and behaviour in between, have been examined in detail, thus suggesting how mixing is affected by modifications to parameters governing the system.

The driven cavity problem consists of a unit two-dimensional cavity with the top wall driven at a prescribed velocity, with the other three remaining stationary. This flow is a well known test problem in computational fluid dynamics, and a complete set of steady solutions at

low Reynolds number ($Re \leq 10,000$) have been obtained by Ghia *et al.* (1982) which concentrated on vortex dynamics. Many have used this problem in the past to benchmark computational schemes (Comini, Manzan and Nonino, 1994, Weinan and Liu, 1994, Hou *et al.* 1995). This study aims to extend the solutions to time-dependent flows at higher Reynolds number where the flow may be periodic, quasi-periodic or chaotic.

Since a global spectral expansion is being used in the numerical scheme, in order to preserve spectral accuracy the top profile is not uniform as in previous studies, but approaches zero smoothly at the two corners. This avoids a discontinuity in the vorticity profile, and hence problems with pressure boundary conditions (Karniadkis *et al.*, 1991). Although any form could be used that satisfies the necessary boundary conditions, the system is changed slightly with each profile. Suggestions for the analytic form can be found in Shen(1990), where he solved the driven cavity up to $Re = 16,000$ with a quartic profile ($16x^2(1-x)^2$) for the moving lid. The solution was steady up to $Re = 10,000$, and between $Re = 10,500$ and $15,000$, the solution appeared to be periodic with one distinct frequency. This was shown by plots of total kinetic energy and velocity at arbitrary locations as a function of time and was attributed to a Hopf bifurcation in the interval (10,000,10,500]. The system becomes quasi-periodic with two distinct frequencies above $Re = 15,500$ and this was also attributed to another bifurcation between (15,000,15,500]. More uniform profiles can be expected to lower these values, and so Liffman(1996) also observed a quasi-periodic behaviour at $Re = 10,000$ with a constant lid profile that exponentially decays at the edges ($1-\exp(-20(1-x^2))$). Verstappen, Wissink and Veldman(1993) analysed the time series of energy dissipation and concluded that the system is chaotic at $Re = 22,000$.

The aim of this paper is to characterise the flow regimes from initial unsteadiness to chaos. Using a passive concentration field, it will be shown that there is an improvement in mixing in the chaotic regime. The mathematical formulation and the boundary conditions will be presented in Section 2. In Section 3, the numerical scheme will be described including the spatial and temporal discretization. The different flow regimes, the methods used to determine chaotic behaviour and their effects on mixing will be presented in Section 4.

2. MATHEMATICAL FORMULATION

The formulation is based on the non-dimensionalised incompressible Navier-Stokes equations, namely :

$$\frac{\partial \mathbf{u}}{\partial t} = -(\mathbf{u}\cdot\nabla)\mathbf{u} - \nabla p + \frac{1}{Re}\nabla^2\mathbf{u} \text{ in } \Omega \quad (1)$$

$$\nabla.\mathbf{u} = 0 \text{ in } \Omega. \quad (2)$$

The two dimensional unit cavity has three stationary boundaries and a 'driving' lid with a fixed velocity :

$$\mathbf{u} = ((1-\exp(-20(1-x^2)))^3, 0). \quad (3)$$

The lid profile used is similar to Liffman(1996), but modified to ensure that both the first derivative and second derivative are continuous at the corners. This profile is used because it is a reasonable approximation to the uniform lid driven cavity, and eliminates the corner singularities. The initial flow velocity is set to be zero throughout the domain. Ramping up the lid smoothly in time or

impulsively starting it does not effect the final flow state.

The passive concentration field is governed by a nondimensional advection-diffusion equation (Toussaint, Carriere and Raynal, 1995),

$$\frac{\partial c}{\partial t} = -(\mathbf{u}\cdot\nabla)c + \frac{1}{Pe}\nabla^2 c \text{ in } \Omega, \quad (4)$$

with a vanishing concentration flux on the solid boundaries,

$$\nabla c \cdot \mathbf{n} = 0 \text{ on } \Gamma. \quad (5)$$

In this closed domain, conservation arguments demand that the spatial intergral of the concentration field remains constant in time. Therefore the condition to remove the non-uniqueness caused by the arbitrary additive constantin the solution of (4) and (5) is

$$\int_\Omega c\ dA - \int_\Omega c_0\ dA = 0, \quad (6)$$

where c_0 is the initial concentration field. In the current work, this is given by

$$c_0(x,y) = \exp(-20((x-0.75)^2+(y-0.25)^2))$$

$$\text{in } \Omega, \quad (7)$$

which will be a concentrated circular region with a maximum of 1.0 and centered at $(0.75, 0.25)$. The diffusivity of the concentration field and the flow field are chosen to be equal ($Pe = Re$).

3. NUMERICAL TECHNIQUE

Previous mixing simulations (Souvaliotis *et al.*, 1995) have demonstrated that false predictions of mixing may result from numerical errors, especially in the chaotic regime. Therefore, the spatial variables are handled by a spectral expansion. As the flow is wall bounded, Chebyshev polynomials (Canuto *et al.*, 1988) are used in each direction within the flow. These are chosen because of the natural compression of the grid around the bounding walls when Gauss-Labotto points are used. Although a Fast Fourier Transform for derivative calculations exists, direct multiplication using optimised matrix routines are faster (Shen, 1991). The increase in calculations still outweights the transform because of its logical operations. Implicit steps are solved using a matrix diagonalisation technique (Canuto *et al.*, 1988).

The time stepping is a modified version of the operator-splitting used within previous spectral element simulations (Karniadakis *et al.*, 1991). The modifications are necessary to facilitate the use of a Runge-Kutta scheme for the convection term. The derivatives in the Navier-Stokes equations have no explicit dependence on t, and therefore a more memory efficient Runge-Kutta scheme can be used (Jameson *et al.*, 1981). The pressure is solved implicitly and the diffusion treated with a Crank-Nicholson scheme. The algorithm for the modified scheme is :

Set $\mathbf{u} = \mathbf{u}^n$
For $k = s, 1, -1$
$\frac{\mathbf{u}^* - \mathbf{u}^n}{\Delta t/k} = -\mathbf{u}\cdot\nabla\mathbf{u}$
$\frac{\mathbf{u}^{**} - \mathbf{u}^*}{\Delta t/k} = -\nabla p \qquad \nabla\cdot\mathbf{u}^{**} = 0$
$\frac{\mathbf{u} - \mathbf{u}^{**}}{\Delta t/k} = \frac{1}{2\ Re}(\nabla^2\mathbf{u} + \nabla^2\mathbf{u}^n)$
End For
Set $\mathbf{u}^{n+1} = \mathbf{u}$

with s being the order of the Runge-Kutta scheme. Fourth order ($k = 4$) is used for all these simulations.

The passive concentration field is solved on the same mesh as the Navier-Stokes equations. A similar operator-splitting technique is used for the passive concentration field. The algorithm is as thus :

Set $c = c^n$
For $k = s, 1, -1$
$\frac{c^* - c^n}{\Delta t/k} = -\mathbf{u}^{n+1} \cdot \nabla c$
$\frac{c - c^*}{\Delta t/k} = \frac{1}{2\ Pe}(\nabla^2 c + \nabla^2 c^n)$
End For
Set $c^{n+1} = c$
in this case.

Measurement of time variations of the total kinetic energy gives a global perspective of the flow. This method has been used by many including Shen (1990) and Liffman(1996) when studying this problem. The total kinetic energy is given by :

$$E(n\Delta t) = \frac{1}{2} \sum_{i,j=0}^{N-1} A_{i,j}[(u_{i,j}^n)^2 + (v_{i,j}^n)^2], \quad (8)$$

where $A_{i,j}$ is the local area around the point (x_i, y_j).

4 RESULTS AND DISCUSSION

4.1 Flow Regimes

The simulations were carried out with 80 nodes in each direction, and a Δt of 0.0025 time units. A steady solution is attainable up to $Re = 8,000$. This was judged after a long settling time of approximately 5,000 time units, where the fluctuations in kinetic energy were less than 0.0001 per cent and the fluctuations in velocity were of the same order as the numerical error.

Between $Re = 8125$ and 9750, the total kinetic energy shows that the system appears to be perfectly periodic, with a period of approximately 2.25 time units. The mean kinetic energy decreases linearly in this range with increasing Reynolds number. This is similar to the observation by Shen(1990) in the first bifurcation region of the regularised driven cavity. The decrease in mean total kinetic energy also extends to higher Reynolds numbers as shown in Figure 1.

Simulations were then performed with increasing Reynolds number. At $Re = 10,000$ and $11,000$, the system would exhibit a quasi periodic state with two dominant frequencies. The dominant periods at $Re = 10,000$ are 2.32 and 3.85, and are 3.76 and 6.40 at $Re = 11,000$. Shen(1990) also observed a two-periodic state when the Reynolds number increased past the perfectly periodic regime. The plot of kinetic energy at $Re = 10,000$ as a function of time is very similar to that obtained by Liffman(1996).

The system appears to settle down to one frequency between $Re = 12,000$ and $13,000$ with a period of oscillation of 1.47. At $Re = 14,000$ and $14,500$, another quasi periodic regime with dominant periods of 1.52 and 15.06 is observed. The system settles down to a periodic cycle at $Re = 15,000$ and $15,500$ with a period of 1.56. Figure 1 shows the kinetic energy trace at several Reynolds numbers illustrating the switching between periodic to quasi-periodic states. The step-wise change in periods is summarised in Figure 2. From $Re = 15,750$ onwards, there is an increase in the number of modes especially at longer periods shown by the spectral plots in Figure 3. This then leads to chaotic features detectable at $Re = 17,000$ and $20,000$.

Each simulation is integrated until the total kinetic energy reached an asymptotic state. For the periodic states, the sinusoidal signal is ensured to be symmetrical for at least 50 cycles. In the quasi-periodic and chaotic states, the requirements are that the mean is constant and the Fourier transform of the kinetic energy signal is constant when taken over

several time periods. This would typically require several thousand time units. The solution at the next lower Reynolds number is used as initial conditions for the simulations. Observations of fluctuations of velocity components at arbitrary locations in the cavity show similar behaviour to the total kinetic energy. Simulations were carried out at a resolution of 100 nodes in each direction at $Re = 14{,}000$, $17{,}000$ and $20{,}000$. The features in the flow field and the behaviour of the total kinetic energy are consistent for both resolution.

4.2 Test for Chaos

Once the flow has reached an asymptotic state, a small disturbance is introduced into the system. The perturbed and unperturbed solutions are then integrated forward in time. The L2 norm of the difference in velocity fields is measured as a function of time to determine if the solutions diverged exponentially to different states. This is typical of chaotic type behaviour (Lorenz, 1963). The perturbation is introduced to the velocity field by

$$\mathbf{u}' = \mathbf{u} + \epsilon f(x, y). \tag{9}$$

The size of the perturbation is chosen to be very small, $\epsilon = 0.0001$ and $f(x, y)$ is chosen so that the resultant flow field satisfies the boundary conditions and continuity. Here it is chosen to be

$$f(x,y) = (2.0\ \sin(2\pi x)\ \cos(2\pi x)\ \sin^2(2\pi y),$$
$$-2.0\ \sin(2\pi y)\ \cos(2\pi y)\ \sin^2(2\pi x)) \text{ in } \Omega. \tag{10}$$

The initial L2 norm was 4.2736×10^{-7}.

This test was done at $Re = 10{,}000$, $17{,}000$ and $20{,}000$. At $Re = 10{,}000$, the L2 norm between the two solutions remained at the same order as the initial value. Integrating these two solutions for 200 time units showed no indications of divergence. At $Re = 17{,}000$, the solutions initially remained close (L2 norm remained of the same order), but after 50 time units the solution rapidly diverged to different states. The L2 norm increased by several orders of magnitude in this time. This was also the case at $Re = 20{,}000$, but the solutions started diverging rapidly at 40 time units after the perturbations were introduced. Therefore the solutions at $Re = 17{,}000$ and $20{,}000$ exhibit chaotic features.

4.3 Passive Concentration Field

Once the flow has reached an asymptotic state, the initial condition for the passive concentration field is introduced. The simulations were then integrated forward 50 time units allowing the passive concentration field to be convected and diffused with the flow field. This was done for $Re = 8000$, $10{,}000$, $14{,}000$, $17{,}000$ and $20{,}000$. At $Re = 8000$ and $10{,}000$, the passive concentration field is convected around the cavity and the dispersion is dominated by diffusion. There is less diffusion of the concentration field at $Re = 14{,}000$, $17{,}000$ and $20{,}000$. There are distortions to the contour lines at $Re = 17{,}000$ which are attributed to the chaotic nature of the flow. At $Re = 20{,}000$, there is significantly more stretching and distorting of the passive concentration field. This suggests that in the chaotic region, convective forces will tend to stretch and distort the fluid.

5. CONCLUSION

The driven cavity, in this case, is steady untill $Re = 8{,}000$. Between $Re = 8{,}125$ and $15{,}500$, the flow switches between a periodic and a quasi periodic state

with a step-wise decrease in period with increasing Reynolds number. Increasing past $Re = 15,750$, there is an increasing number of modes until the system appears to be chaotic at $Re = 17,000$.

Once the flow has reached an asymptotic state, a small perturbation introduced to the solutions at $Re = 17,000$ and $20,000$ caused the system to diverge exponentially from the unperturbed state. This is typical of chaotic behaviour where small changes lead to the formation of seperate differing states. Mixing is improved in the chaotic region by stretching and distortion of fluid elements.

ACKNOWLEDGMENTS

The first author (B.T.T.) acknowledges the financial support of the Overseas Postgraduate Research Scholarship and the Monash Graduate Scholarship. The granting of computing time from the Monash High Performance Computer facility that allowed the simulations to be performed is also gratefully acknowledged.

REFERENCES

Comini, G., Manzan, M. and Nonino, C., (1994), "Finite Element Solution of the Streamfunction-Vorticity Equations for Incompressible Two-Dimensional Flows", *Int. J. Num. Methods Fluids*, **19**, 513-525.

Canuto, C., Hussaini, M.Y., Quarteroni, A. and Zang, T.A., (1988), *Spectral methods in fluid dynamics*, Springer-Verlag.

Ghia, U., Ghia, K.N., and Shin, C.T., (1982), "High-Re solutions for incompressible flow using the Navier-Stokes equations and a multi-grid", *J. Comp. Phys.*, **48**, 387-411.

Hou, S., Zou, Q., Chen, S., Doolen, G. and Cogley, A.C., (1995), "Simulation of Cavity Flow by the Lattice Boltzmann Method", **118** 329-347.

Jameson, A., Schmidt, H. and Turkel, E., (1981), "Numerical Solutions of the Euler Equations by Finite Volume Methods Using Ringe-Kutta Time Stepping Schemes", *AIAA* Pap. No 81-1259.

Karniadakis, G.E., Israeli, M. and Orszag, S.A., (1991), "High-Order Splitting Methods for the Incompressible Navier-Stokes Equations", *J. Comp. Phys.*, **97**, 414-443.

Lorenz, E.N., (1963) "Deterministic nonperiodic flow", *J. Atmospheric Sci.*, **20**, 130-141.

Shen, J., (1991), "Hopf Bifurcation of the Unsteady Regularized Driven Cavity Flow", *J. Comp. Phys.*, **95**, 228-245.

Souvaliotis, A., Jana, S.C. and Ottino, J.M. (1995). Potentialities and limitations of mixing simulations. AIChE, **41**, 1605-1621.

Toussaint, V., Carriere, P. and Raynal, F., 1995, "A Numerical Eulerian Approach to Mixing by Chaotic Advection", *Phys. Fluids*, **7**(11), 2587-2600.

Verstappen, R., Wissink, J.G., and Veldman, A.E.P, 1993, "Direct Numerical Simulation of Driven Cavity Flows", *App. Sci. Res.*, **51**, 377-381.

Weinan, E. and Liu J., (1996), "Essentially Compact Schemes for Unsteady Viscous Incompressible Flows", *J. Comp. Phys.*, **126**, 122-138.

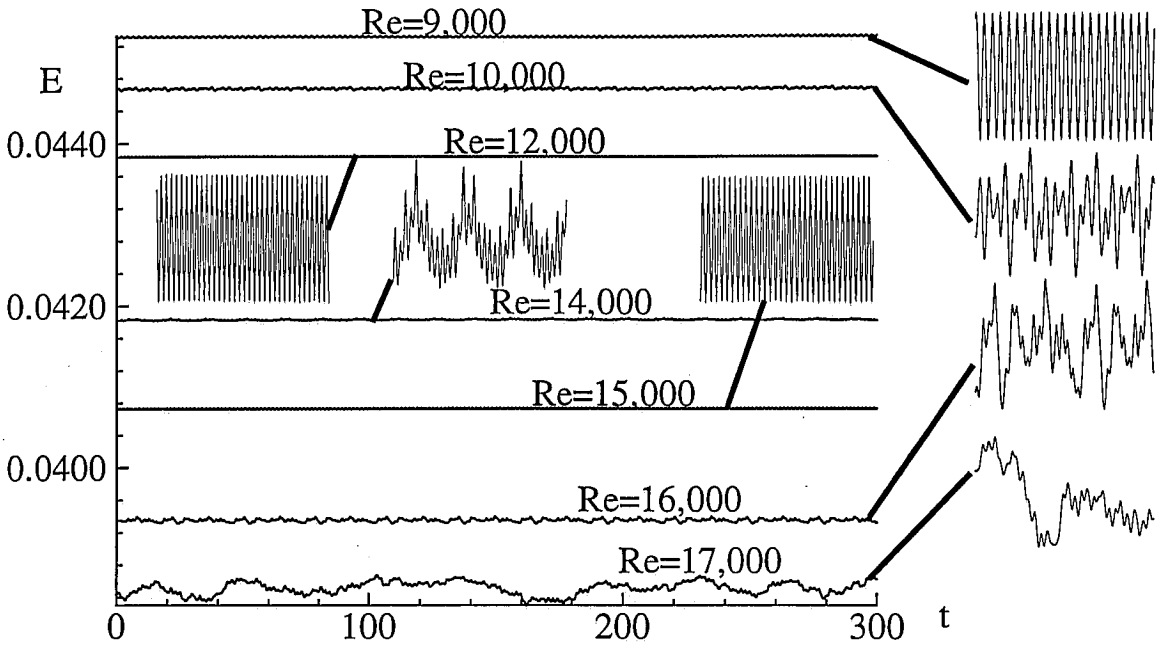

Figure 1 : Total kinetic energy trace for 300 time units at several Reynolds numbers. Traces are taken when an asymptotic state has been reached. Inserts show 50 time units of detailed behaviour at each Re.

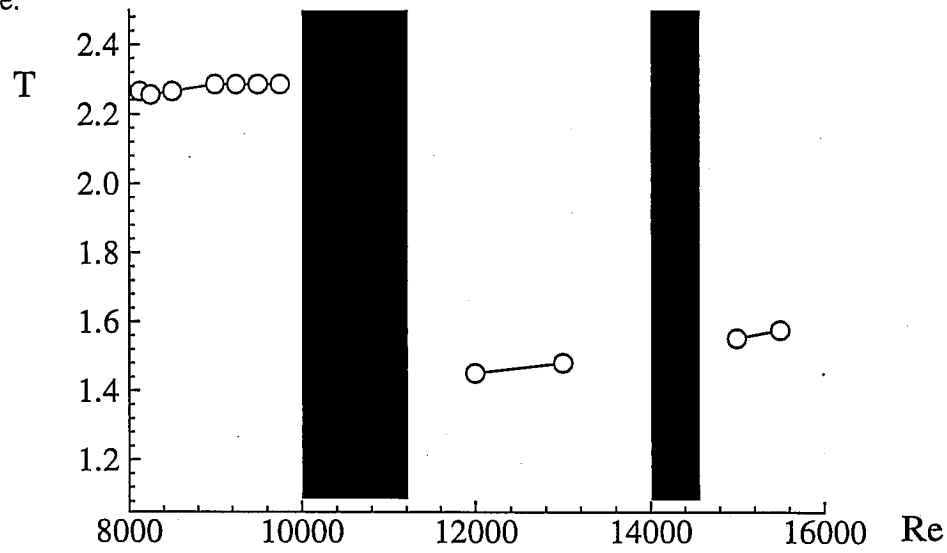

Figure 2 : Period of oscillation as a function of Reynolds number. Shaded regions exhibit quasi-periodic behaviour.

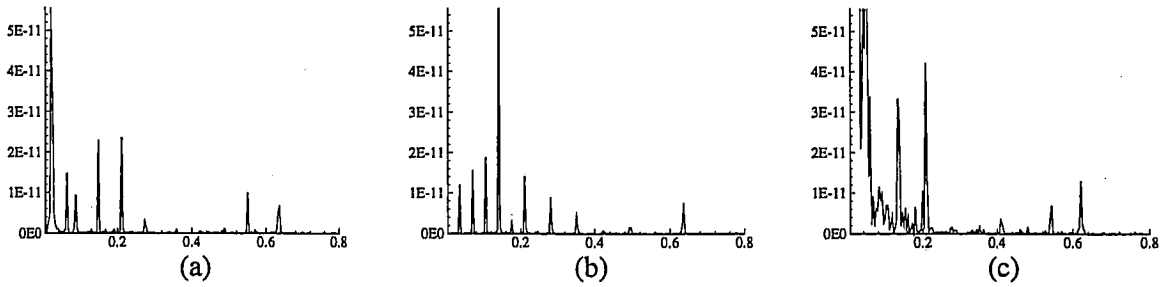

Figure 3 : Spectral plot of kinetic energy at (a) Re=15,750, (b) Re=16,000 and (c) Re=17,000 showing increasing spectral modes at the transition to chaos.

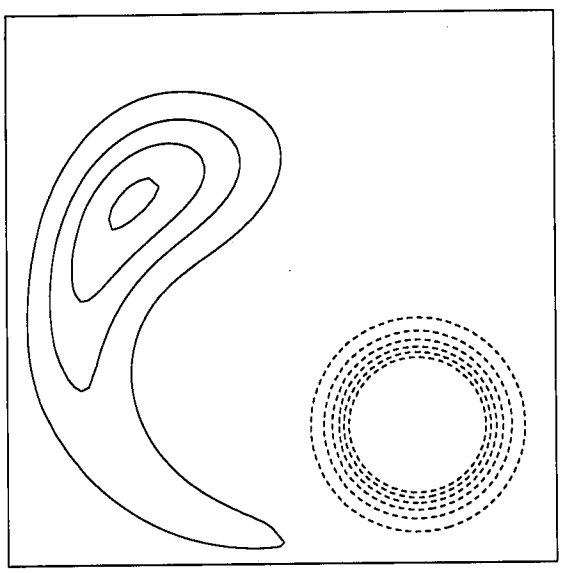

(a)

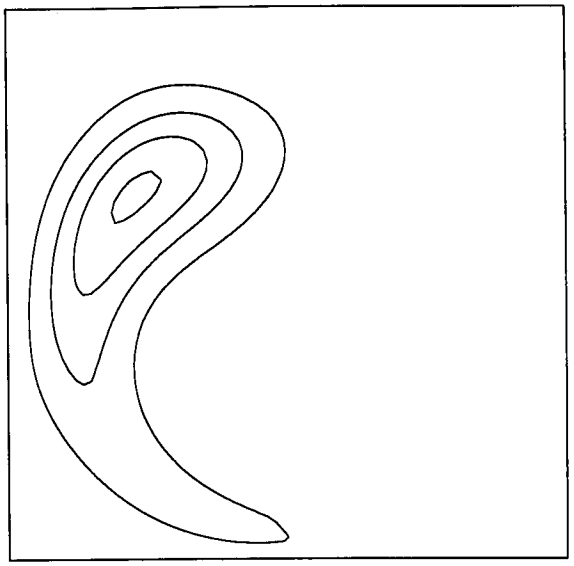

(b)

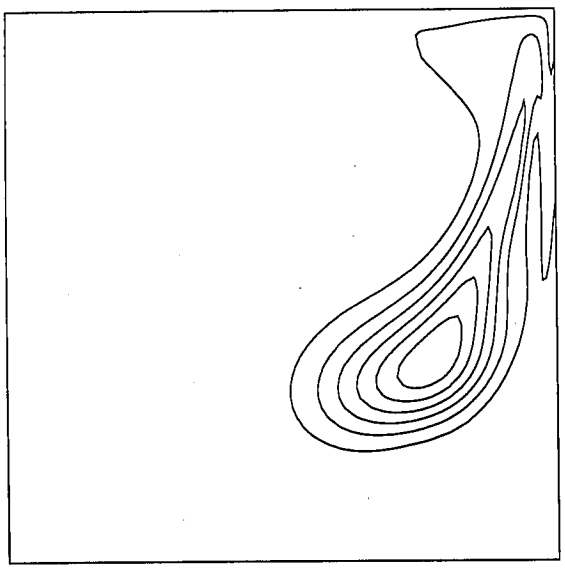

(c)

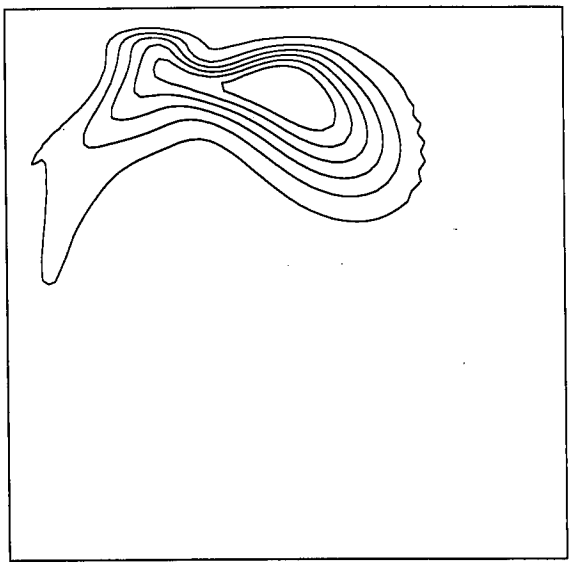

(d)

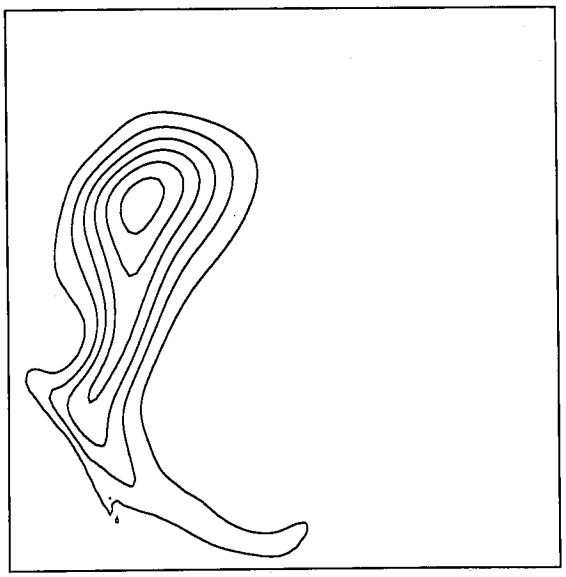

(e)

Figure 4 : Contours of passive concentration field 50 time units after introduction to the asymptotic flow state at (a) Re = 8,500, (b) Re = 10,000, (c) Re = 14,000 , (d) Re = 17,000, (e) Re=20,000 . Contour levels are at 0.05, 0.10, 0.15, 0.20, 0.25 and 0.30. The 'driving' lid is at the top and the direction is towards the right of the page. Dashed lines in (a) represent the initial scalar field.